Articles

Structural Basis of Phospholipase A_2 Inhibition for the Synthesis of Prostaglandins by the Plant Alkaloid Aristolochic Acid from a 1.7 Å Crystal Structure[†,‡]

Vikas Chandra,[§] Jayasankar Jasti,[§] Punit Kaur,[§] A. Srinivasan,[§] Ch. Betzel,[||] and T. P. Singh*[,§]

Department of Biophysics, All India Institute of Medical Sciences, New Delhi 110029, India, and Institute of Medical Biochemistry and Molecular Biology, UKE. C/O DESY, Notkestrasse 85, 22603 Hamburg, Germany

Received March 22, 2002; Revised Manuscript Received July 5, 2002

ABSTRACT: This is the first structural observation of a plant product showing high affinity for phospholipase A_2 and regulating the synthesis of arachidonic acid, an intermediate in the production of prostaglandins. The crystal structure of a complex formed between *Vipera russelli* phospholipase A_2 and a plant alkaloid aristolochic acid has been determined and refined to 1.7 Å resolution. The structure contains two crystallographically independent molecules of phospholipase A_2 in the form of an asymmetric dimer with one molecule of aristolochic acid bound to one of them specifically. The most significant differences introduced by asymmetric molecular association in the structures of two molecules pertain to the conformations of their calcium binding loops, β-wings, and the C-terminal regions. These differences are associated with a unique conformational behavior of Trp^{31}. Trp^{31} is located at the entrance of the characteristic hydrophobic channel which works as a passage to the active site residues in the enzyme. In the case of molecule A, Trp^{31} is found at the interface of two molecules and it forms a number of hydrophobic interactions with the residues of molecule B. Consequently, it is pulled outwardly, leaving the mouth of the hydrophobic channel wide open. On the other hand, Trp^{31} in molecule B is exposed to the surface and moves inwardly due to the polar environment on the molecular surface, thus narrowing the opening of the hydrophobic channel. As a result, the aristolochic acid is bound to molecule A only while the binding site of molecule B is empty. It is noteworthy that the most critical interactions in the binding of aristolochic acid are provided by its OH group which forms two hydrogen bonds, one each with His^{48} and Asp^{49}.

Extracts of several plants are used in folk medicine as snake venom antidotes. Aristolochic acid (9-hydroxy-8-methoxy-6-nitrophenanthro(3,4-d)-1,3-dioxole-5-carboxylic acid), an alkaloid from *Aristolochia* sp. (*1*), has been shown to interact with several venom toxins and enzymes such as phospholipase A_2 (PLA_2)[1] (*2*). PLA_2 (EC 3.1.1.4) mediates hydrolysis of fatty acids, especially arachidonate, from the *sn*-2 position of membrane phospholipids. It is significant because it is the rate-limiting step in the liberation of the requisite substrate for the biosynthesis of eicosanoids (*3*), which have been implicated in the pathogenesis of inflammatory diseases (*4*, *5*). It has been reported that aristolochic acid inhibits PLA_2 in vitro and also decreases edema induced by snake venom or human synovial fluid PLA_2 (*2*, *6*). So far, the actual mode of binding of aristolochic acid to PLA_2 is not known. In view of such potent applications, a detailed knowledge of aristolochic acid binding to PLA_2 at the molecular and structural levels will provide the necessary lead for the design of specific inhibitors of PLA_2. We report here the detailed three-dimensional structure of the complex formed between PLA_2 from the venom of *Daboia russelli pulchella* (PLA_2) and aristolochic acid at 1.7 Å resolution. The structure reveals the details of specific binding of aristolochic acid to PLA_2 and specific conformational changes in PLA_2 when it binds to aristolochic acid.

EXPERIMENTAL PROCEDURES

Purification of PLA_2. PLA_2 was purified from crude venom of *D. russelli pulchella*. The venom was obtained from Irula Snake Catchers Industrial Society Limited (Chennai, India). The purification procedure was developed by us as reported earlier (*7*). It involves an affinity step on Cibacron blue matrix and ion exchange chromatography on CM Sephadex C-25. The purity was checked by SDS−PAGE.

[†] This work was financially supported by the Department of Science and Technology, India. J.J. thanks the Council of Scientific and Industrial Research, New Delhi, for the award of a fellowship. C.B. thanks DFG for Grant BE 1443/9-1.

[‡] The atomic coordinates have been deposited in the Protein Data Bank as entry 1FV0.

* To whom correspondence should be addressed. Phone: +91-11-653 3931. Fax: +91-11-686 2663. E-mail: tps@aiims.aiims.ac.in.

[§] All India Institute of Medical Sciences.

[||] Institute of Medical Biochemistry and Molecular Biology.

[1] Abbreviations: CMC, critical micelle concentration; DTNB, 5,5′-dithiobis(2-nitrobenzoic acid); DLS, dynamic light scattering; PDB, Protein Data Bank; PLA_2, phospholipase A_2; rms, root-mean-square; R_H, hydrodynamic radius; SDS−PAGE, sodium dodecyl sulfate−polyacrylamide gel electrophoresis.

10.1021/bi0258593 CCC: $22.00
Published on Web 08/14/2002

Kinetics and Inhibition Studies of PLA_2 with Aristolochic Acid. The purified enzyme was used for kinetics studies. To determine the inhibitory potency of aristolochic acid, the value of its inhibitor constant (K_i) was estimated. In the kinetics experiments, the 1,2-dithio analogue of diheptanoylphosphatidylcholine with a CMC value of 4×10^{-4} M (*8*) was used as a substrate (PLA_2 assay kit, Cayman Chemicals, Ann Arbor, MI). Upon hydrolysis of the thio ester bond at the *sn*-2 position by PLA_2, free thiols were liberated which were detected using 5,5′-dithiobis(2-nitrobenzoic acid) (DTNB). All assays were performed in 20 mM sodium cacodylate buffer at pH 7.0 and 25 °C. The enzyme concentration was fixed at 1.5 μM, while substrate concentrations were varied from 0.5 to 2.0 mM. PLA_2 was incubated separately with 0.5, 1.0, and 1.5 μM aristolochic acid for 30 min. The reactions were initiated by addition of 0.5, 0.7, 1.0, 1.4, and 2.0 mM substrate for each inhibitor concentration, and the amounts of resulting products were estimated by the differences in absorbance at 414 nm. In separate experiments, inhibitory assays with 1:0.25, 1:0.5, 1:1, 1:10, and 1:20 molar ratios of enzyme and aristolochic acid were also carried out.

Dynamic Light Scattering (DLS). As reported earlier (*9*), two molecules of PLA_2 were found to be associated in the crystalline state and were expected to be in association in solution as well. To establish this assumption, the experiments on the size distribution of PLA_2 molecules were carried out using a dynamic light scattering system (Dierks & Partner, Hamburg, Germany), and the data that were generated were analyzed using Schulze software (*10*). The sample solutions were prepared in sodium cacodylate buffer (20 mM, pH 6.5) made with water prepared with a Millipore Alpha-Q system. To eliminate dust and other large particles, all samples were further filtered on 0.1 μm polyvinylidene difluoride filters (Millipore) prior to measurements. PLA_2 concentrations were varied from 0.05 to 20 mg/mL at a constant temperature of 25 °C. Samples were manually injected into the flow cell (50 μL) and illuminated with a 25 mW, 600 nm solid state laser. Data were collected in five replicas for each measurement.

Crystallization. To determine the structural basis of the binding of aristolochic acid to PLA_2, the crystals of the complex formed between PLA_2 and aristolochic acid were required. A molecule of aristolochic acid contains four aromatic rings with additional substitutions at four sites that make it a large molecule for soaking experiments. In view of this, the cocrystallization of PLA_2 with aristolochic acid was attempted. The purified PLA_2 was dissolved in 10 mM sodium cacodylate buffer (pH 7.0) to a final protein concentration of 15 mg/mL. To it was added aristolochic acid in excess molar concentrations. The mixture was incubated for 24 h, and then 20 μL drops of the above mixture were set up in the hanging drop vapor diffusion method with a reservoir containing 1.2 M ammonium sulfate, 1 mM $CaCl_2$, and 3% dioxane in the same buffer. Yellow-colored crystals with dimensions of up to 0.5 mm × 0.3 mm × 0.3 mm were obtained in 7−8 days.

Data Collection. The crystals of the complex were stabilized in 20% glycerol as a cryoprotectant for data collection at low temperatures. A single crystal was mounted in a nylon loop and flash-frozen in a nitrogen stream at 100 K. The crystals diffracted to 1.7 Å resolution. The data were collected on EMBL beamline X-11 at DESY (Hamburg, Germany) with a λ of 0.98 Å using a MAR 345 imaging plate scanner with 1.0° rotation for each image. The data were processed using DENZO and SCALEPACK (*11*). The results of the data collection and processing are given in Table 1.

Table 1: Crystallographic Data

PDB entry	1FV0
space group	$C222_1$
unit cell dimensions (Å)	
a	76.05
b	89.48
c	76.87
data collection	
resolution limit (Å)	20.0−1.7
no. of observations	419758
no. of unique reflections	28922
completeness[a] (%)	99.1 (97.9)
R_{sym}[a,b]	0.045 (0.034)
refinement	
R_{cryst} [c]	0.184
R_{free}[d]	0.201
no. of protein atoms	1888
no. of aristolochic acid atoms	26
no. of sulfate ions	4
no. of glycerol atoms	12
no. of dioxane atoms	12
no. of acetate ions	1
no. of water molecules	315
rms deviation from ideal values	
bond lengths (Å)	0.007
bond angles (deg)	1.3
dihedral angles (deg)	21.5
residues in the most allowed regions of Ramachandaran map (%) (*21*)	90.3

[a] Values in parentheses correspond to the highest-resolution shell (1.73−1.70 Å). [b] $R_{sym} = \sum|I(h_i) - \langle I(h)\rangle|/\sum\langle I(h_i)\rangle$, where $I(h_i)$ is sealed intensity of the *i*th symmetry-related observation of reflection *h* and $\langle I(h)\rangle$ is the mean value. [c] $R_{cryst} = \sum|F_o(h) - F_c(h)|/\sum F_o(h)$, where $F_o(h)$ and $F_c(h)$ are the observed and calculated structure factor amplitudes for reflection *h*, respectively. [d] R_{free} was calculated against 5% of the complete data set excluded from the refinement.

Structure Determination and Refinement. The structure was determined by a molecular replacement method using the model of PLA_2 previously obtained at 1.9 Å resolution (*12*). The structure contains two molecules designated as A and B, which were refined independently. The refinement was carried out using the program CNS (*13*). The $2F_o - F_c$ and $F_o - F_c$ maps were calculated to adjust the protein molecule in the density maps using the program O (*14*). The resolution was extended stepwise from 3.0 to 1.7 Å. Several cycles of restrained positional refinement with individual *B*-factors and several rounds of simulated annealing from 3000 to 300 K allowed the correct tracing of the flexible loops where the conformations were markedly different from the initial model. At the end of this stage, the *R*-factor dropped to 0.227 and R_{free} was 0.271. Both Fourier ($2F_o - F_c$) and difference Fourier ($F_o - F_c$) maps computed at this stage clearly indicated the presence of aristolochic acid in the binding site of molecule A (Figure 1). However, there was no density for aristolochic acid in the corresponding binding region of molecule B. This was indeed an unexpected result. The repeated calculations using various cutoffs at different stages of refinement also did not show any density, indicating the absence of aristolochic acid in molecule B. Further rigid body refinement and several rounds of posi-

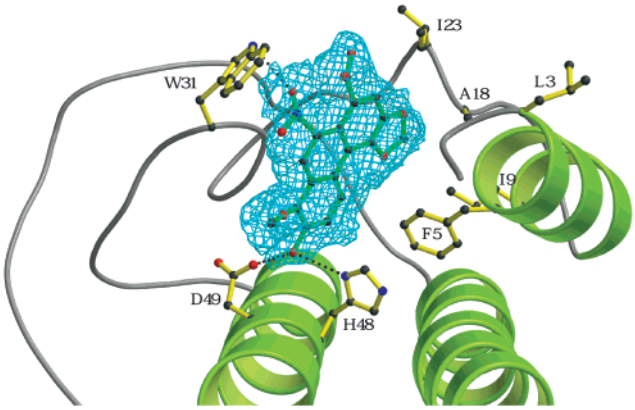

FIGURE 1: Difference $F_o - F_c$ map contoured at 2.5σ showing the presence of aristolochic acid at the binding site of molecule A.

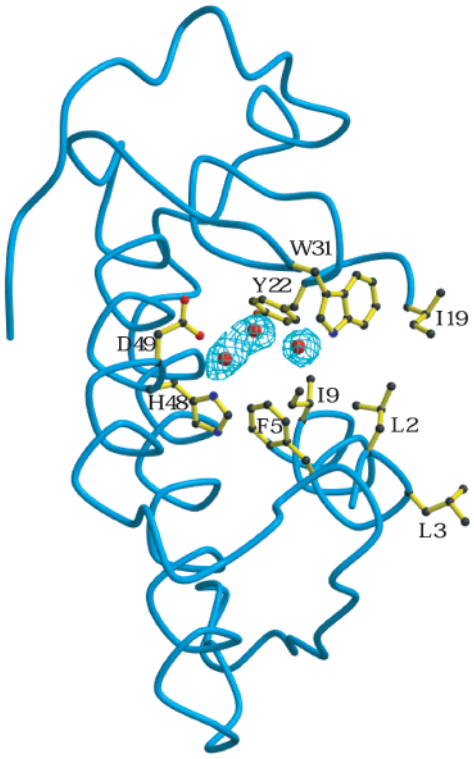

FIGURE 2: Difference $F_o - F_c$ map showing the presence of three water molecules in the hydrophobic channel of molecule B. The contours were drawn at 2.5σ.

tional and restrained individual *B*-factor refinement were subsequently performed. At the end of this stage, some missing side chains appeared more clearly and the density for aristolochic acid in molecule A improved considerably. Some additional peaks above 3σ in $F_o - F_c$ and 1σ in $2F_o - F_c$ electron density maps were interpreted as four sulfate ions, two dioxanes, two glycerols, and an acetate ion according to the shapes of the electron densities as well as the compatibilities of the protein residues surrounding them for attractive interactions. These maps were also used to determine the positions of 315 water molecules. It may be noted that three of these water molecules were located in the hydrophobic channel of molecule B (Figure 2). It may also be mentioned here that 1 mM $CaCl_2$ was added to the protein solution in the crystallization setups, but there was no clear density for the calcium ion in the structure; hence, it was not included in the refinement. After a final round of

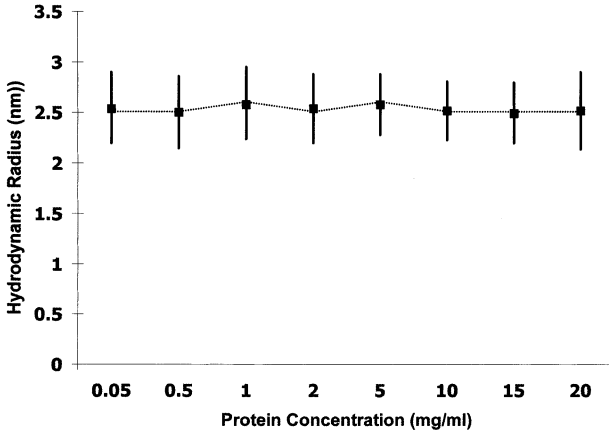

FIGURE 3: Hydrodynamic radii (R_H) of PLA_2 as a function of protein concentration (milligrams per milliliter) in 20 mM sodium cacodylate buffer (pH 6.5). The values remain constant over the concentration range from 0.05 to 20.0 mg/mL.

3000 K simulated annealing coupled with positional refinement and restrained individual *B*-factor refinement, the *R*-factor was 0.184 (R_{free} = 0.201). The coordinates have been deposited in the Protein Data Bank (entry 1FV0).

RESULTS AND DISCUSSION

Inhibition of PLA_2 by Aristolochic Acid. The purified samples of PLA_2 indicated a molecular mass of 14 kDa on SDS−PAGE. However, the results of DLS using uncomplexed samples of PLA_2 showed that the mean hydrodynamic radius (R_H) of PLA_2 in the protein concentration range from 0.05 to 20 mg/mL was 2.54 nm. The molecular mass corresponding to the above hydrodynamic radius was estimated to be 28 kDa (*15*, *16*). The polydispersity values in these estimations were <15% of the average radius, indicating that all the PLA_2 molecules existed in the dimeric form in solution (Figure 3). It may be noted that the approximate radii calculated from the crystal structure for the monomer and dimer were ~1.1 and 2.2 nm, respectively. Furthermore, the gel filtration profile of this protein also suggested a molecular mass of 28 kDa. Therefore, it was assumed that the two molecules of this PLA_2 existed in association in the solution state.

The percentage inhibition values of PLA_2 for inhibition by aristolochic acid at different molar ratios (1:0.25, 1:0.5, 1:1, 1:10, and 1:20) of enzyme to aristolochic acid were estimated. It was observed that at all these concentrations of aristolochic acid, the levels of inhibition were always less than 50% (Figure 4). The detailed kinetic experiments carried out with aristolochic acid showed that it was a competitive inhibitor of PLA_2 with a K_i value of 1.18 ± 0.08 μM. The calculated K_M value for the substrate was found to be 0.69 mM. The higher concentrations of aristolochic acid were expected to show higher levels of inhibition. However, the level of inhibition did not exceed 50% irrespective of the concentrations of the aristolochic acid, thereby suggesting that the binding sites of the 50% PLA_2 molecules were either not accessible or not suitable for binding to aristolochic acid. On the other hand, as indicated by the data from the experiments with controls, the enzyme activity in the absence of aristolochic acid was found to be 100% (Figure 4). Since the two molecules of PLA_2 were associated and only 50% of them were bound to aristolochic acid while the substrate

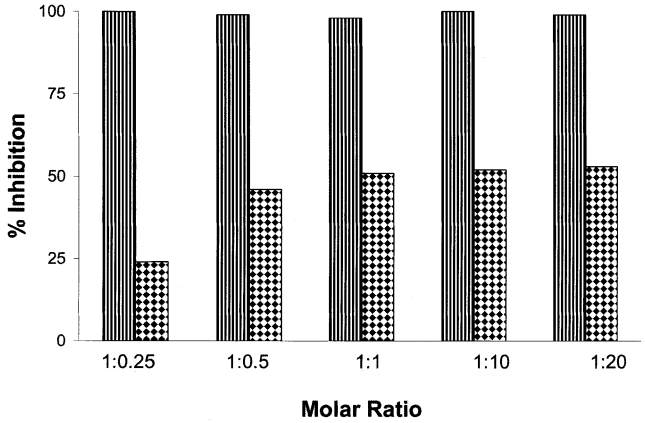

FIGURE 4: PLA_2 activity was measured as described in Experimental Procedures. The enzyme:aristolochic acid ratios that were used were 1:0.25, 1:0.5, 1:1, 1:10, and 1:20. The estimated enzyme activity without aristolochic acid is shown with striped bars and corresponded to 100%, while those for the enzyme with aristolochic at different ratios is shown with checkered bars. The increasing ratios of aristolochic acid did not enhance the level of inhibition beyond 50%.

was found interacting with all the PLA_2 molecules, the effect of association clearly indicated a functional significance. In summation, it suggested two possibilities of enzyme activation. (i) If the association hindered the access to the binding site, the substrate used in these experiments was able to dissociate PLA_2 molecules before binding to it, and (ii) if the conformation of either of the two associated molecules was not suitable for binding, the substrate was able to induce a desirable conformation for binding. Both these effects may cause a slight reduction in the overall activity of the enzyme. It may be noted here that the enzyme activity of this PLA_2 was reported to be slightly lower than that observed in other PLA_2s (*17*, *18*). It is also well-known that PLA_2 enzymes show higher activity with aggregated substrates such as membrane phospholipids (*19*). Since the substrate concentrations were above the critical micellar concentration in the experiments presented here, it presents itself as an aggregated system with a micellar structure. Therefore, due to its aggregated nature, this substrate was capable of creating both effects, i.e., dissociation of two molecules as well as the induction of a required conformation for binding. These actions might not have been possible with monodispersed inhibitors and substrates.

Quality of the Model. The final model consists of two PLA_2 molecules, one molecule of aristolochic acid, and 315 water molecules. The refinement of the final model converged to an *R*-factor of 18.4% and an R_{free} of 20.1% for 28 922 reflections in the resolution range of 20.0−1.7 Å. The protein molecules have geometries close to ideal values with root-mean-square (rms) deviations of 0.007 Å and 1.3° from standard values for bond lengths and angles, respectively. The quality of the model was further checked by PROCHECK (*20*) which showed 90.3% of the non-Gly and non-Pro residues in the most allowed regions of the Ramachandran plot (*21*). The structure of PLA_2 is based on well-defined electron density for both molecules. The aristolochic acid was located in the binding site of molecule A only and had excellent electron density (Figure 1). The corresponding site in molecule B was empty with three sparsely distributed water molecules (Figure 2). The details of the refinement are given in Table 1.

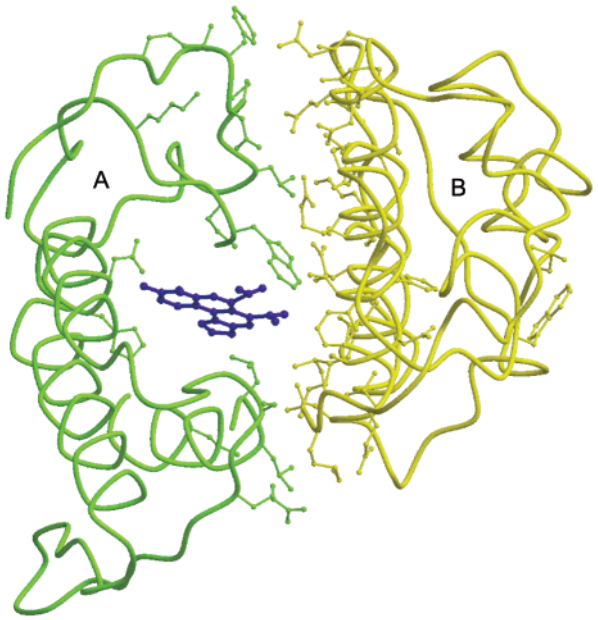

FIGURE 5: Asymmetrical association of molecules A and B showing the long interface. There are three weak direct intermolecular hydrogen bonds and a large number of hydrophobic interactions between molecules A and B. Trp^{31} of molecule A is involved in several hydrophobic interactions. The opening of the channel in molecule B is constrained by the positioning of the Trp^{31} side chain.

Molecular Associations. The structure contains two crystallographically independent molecules A and B which form an asymmetric dimer. The aristolochic acid binds to molecule A while the binding site of molecule B is empty (Figure 5). In the lower region of the dimer, they form three weak intermolecular hydrogen bonds: Leu^2 N (A)···Lys^{131} O (B) (3.5 Å), Leu^3 N (A)···Lys^{131} O (B) (3.4 Å), and Leu^{119} O (A)···Gln^{108} $N^{\epsilon 2}$ (B) (3.1 Å). In addition to those, there are a number of hydrogen bonds through water molecules and hydrophobic interactions covering the whole interface region of the dimer. However, the most striking interactions were observed between Trp^{31} of molecule A and a number of residues from molecule B. As Trp^{31} is located at the mouth of the hydrophobic channel, the effect of these interactions is expected to influence the binding of ligands to the enzyme. Therefore, the absence of calcium in the present structure is perhaps compensated by a number of hydrophobic interactions with Trp^{31}. It may be noted here that Trp^{31} in molecule B is exposed to the surface and is not constrained by the molecular association. Hence, the most notable feature of this asymmetric dimer corresponds to the differences in the conformations of Trp^{31} residues of molecules A and B. The values of torsion angles φ, ψ, χ^1, and χ^2 for Trp^{31} in molecules A and B are −74, −39, −62, and 88° and −131, 169, −59, and −83°, respectively. Despite the above, the overall conformations of molecules A and B are essentially similar with an overall rms difference of 0.8 Å for the C^α positions. There are only three regions comprising the calcium binding loop (residues 25−34), the β-wing consisting of two antiparallel β-strands (residues 74−85), and the C-terminal stretch (residues 119−133) which display significant conformational differences.

It may also be indicated here that the stability of this PLA_2 has been reported to be significantly higher than that observed for other PLA_2s (*22*−*24*). Generally, the PLA_2s exhibit enzymatic activity up to 50 °C, while the present

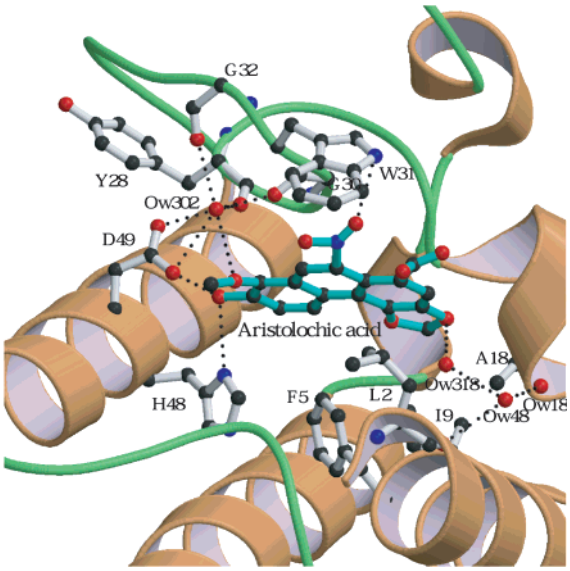

FIGURE 6: Dotted lines represent hydrogen bond interactions of aristolochic acid with PLA_2 in molecule A. The most critical interactions involve $N^{\delta 1}$ of His^{48} and $O^{\delta 1}$ of Asp^{49} with the OH group of aristolochic acid. This figure was drawn with MOLSCRIPT (*25*) and RASTER3D (*26*).

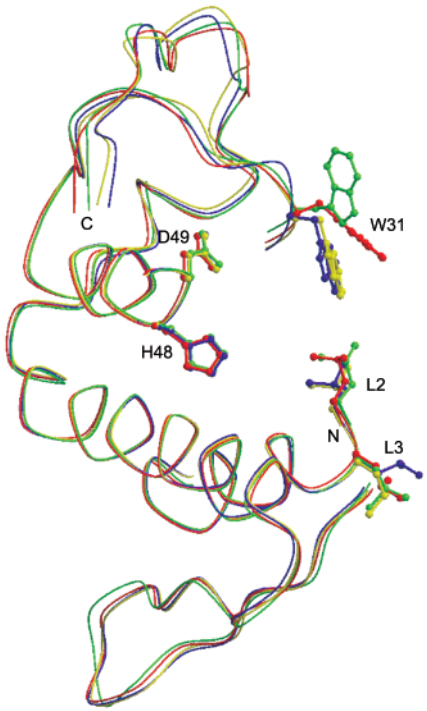

FIGURE 7: Positioning of Trp^{31} vis-à-vis the hydrophobic channel. Molecule B in the native structure of PLA_2 (yellow), molecule B in the complex presented here (blue), molecule A in the complex presented here (red), and molecule A in the native structure (green). The distances between the two nearest atoms of Leu^2 and Trp^{31} from two opposite walls of the hydrophobic channel are 8.3 Å in molecule A of the native structure, 6.6 Å in molecule A of the complex presented here, and 4.7 Å in molecule B for both the native and complex structures.

PLA_2 remains active up to 96 °C. This may presumably be due to its asymmetric molecular association.

Binding of Aristolochic Acid to PLA_2. The electron density for aristolochic acid in molecule A was found to be exceptionally good which allowed a detailed description of the interactions between PLA_2 and aristolochic acid. In the complex, the ligand is placed in the binding site of molecule A with its aromatic moieties occupying the large hydrophobic pocket (Figure 5). The aristolochic acid is oriented in such a way that its only OH group forms two excellent hydrogen bonds with active site residue His^{48} $N^{\delta 1}$ [$N^{\delta 1}\cdots O(H)$, 3.0 Å] and Asp^{49} $O^{\delta 1}$ [$O^{\delta 1}\cdots O(H)$, 2.5 Å]. There are additional hydrogen bonds involving Trp^{31} and three water molecules [OW^{48}, OW^{302}, and OW^{318} (Figure 6)]. The interactions of aristolochic acid with Trp^{31} induce further conformational change in the side chain of Trp^{31}, pulling it slightly toward the hydrophobic channel as compared to the native structure. On the other hand, the corresponding region in molecule B is occupied by only water molecules. Therefore, the conformation of Trp^{31} in molecule B is unaffected by formation of a complex between PLA_2 and aristolochic acid.

Comparison of Structures of PLA_2 in the Complex Presented Here with That in the Native State [PDB Entry 1FB2 (12)]. In both structures, there are two molecules of PLA_2 in the asymmetric unit which are held together asymmetrically. In the structure presented here, molecule A is complexed with aristolochic acid while molecule B has an empty binding site. The most striking difference in the structures of molecule A in its native state (*12*) and in the complex presented here is observed in the orientation of Trp^{31}. When the enzyme binds to aristolochic acid, the side chain of Trp^{31} moves significantly toward the hydrophobic channel. The distance between the nearest atoms of Trp^{31} ($C^{\zeta 2}$) and Leu^2 ($C^{\delta 2}$) has been reduced from 8.3 to 6.6 Å (Figure 7). It is noteworthy that the interactions between molecules A and B involving Trp^{31} of molecule A and the C-terminal residues of both molecules differ considerably (Table 2). The reduced distances in the complex indicate an enhancement in the stability of the dimer in the complexed state. On the other hand, the conformations of molecules B in the two structures were identical and the orientations of Trp^{31} remained unchanged (Figure 7). The distance between the two nearest atoms of Trp^{31} and Leu^2 from two opposite walls of the channel was 4.7 Å in molecule B of both the native and the complex structure. The observed variations in the dispositions of the side chain of Trp^{31} in molecules A and B and in the complex with aristolochic acid indicate a high degree of flexibility in the side chain of Trp^{31}. In an

Table 2: Distances (Å) between the Atoms of Trp^{31} in Molecule A with the Nearest Atoms of Molecule B in the Complex Presented Here and the Native Structure (*12*)[a]

molecule A		molecule B	complex structure	native structure
Trp^{31}	$C^{\delta}-C^{\delta}$	Arg^{43}	3.7	3.8
	$C^{\delta 2}-C^{\delta}$		3.1	3.7
	$C^{\gamma}-C^{\delta}$		3.3	3.8
	$C^{\epsilon 2}-C^{\gamma}$		3.6	5.1
	$N^{\epsilon 1}-C^{\gamma}$		3.9	5.0
	$N^{\epsilon 1}-C^{\gamma 2}$	Val^{47}	3.6	8.5
	$C^{\eta 2}-C^{\delta 2}$	Phe^{46}	3.4	10.0
	$C^{\eta 2}-C^{\epsilon 2}$		3.8	10.4
Leu^2	N−O	Lys^{131}	3.5	4.4
	$C^{\beta}-C^{\beta}$		3.8	6.8
Leu^3	N−O	Lys^{131}	3.4	5.1
	$C^{\delta 2}-C^{\gamma}$		3.4	5.2
	$C^{\beta}-C^{\gamma}$		3.7	5.0
Leu^{119}	$O-N^{\epsilon 2}$	Gln^{108}	3.1	2.9
	$C^{\delta 2}-C^{\alpha}$	Ala^{101}	3.7	4.0

[a] The distances involving the C-terminal regions in both molecules are also given.

independent monomer of the PLA_2 described here, the side chain will occupy a conformation similar to that observed in molecule B and is expected to be stabilized by interactions with the residues of the hydrophobic channel, resulting in closing of the entrance of the hydrophobic channel.

CONCLUSIONS

PLA_2 forms a stable asymmetric dimer, leading to important functional implications. The structure shows that a plant alkaloid aristolochic acid binds to one of the two molecules of the dimer as indicated by kinetics studies. However, both molecules seem to function normally with aggregated or micellar substrates. In the dimer presented here, the entrance to the binding site of molecule A lies at the interface of two molecules while that of molecule B is accessible from the surface. The important conformational variations between molecule A and B were limited to three stretches of the protein chain, i.e., residues 25−34, 74−85, and 119−133. The most visible difference is observed in the conformation of Trp^{31}. The intermolecular hydrophobic interactions involving Trp^{31} of molecule A with the residues of molecule B determine the placement of the side chain of Trp^{31}. As it is part of the calcium binding loop (residues 25−34), Trp^{31} induces a conformational change in the calcium binding loop as a whole with an epicenter at Trp^{31} itself. As influenced by asymmetrical molecular association, the positioning of Trp^{31} in molecule A acquires a suitable conformation for ligand binding. Although the opening of the channel in molecule A is located at the interface, the affinity of the binding site, dimensions of the hydrophobic channel, and accessibility via the interface are suitable for the binding of monodispersed ligands such as aristolochic acid. On the other hand, in the absence of a strong hydrophobic environment, the hydrophobic channel of molecule B attracts its Trp^{31} toward it, leading to the closing of the entrance to the hydrophobic channel. Therefore, despite the accessibility of the binding site in molecule B, the inhibitor was unable to bind to it due to the narrow opening to the channel. The results of kinetics studies, the influence of hydrophobic interactions on the conformations of Trp^{31}, and the asymmetric association which is predominantly stabilized by hydrophobic interactions clearly indicate that the aggregated micellar substrates were capable of both inducing a suitable conformation in molecule B and dissociating molecule A and B for binding to the enzyme. The monodispersed molecules having high affinities for the binding site of PLA_2 are capable of diffusing through the interface to bind the molecule. However, they are unable to induce a suitable conformation, thus failing to bind to molecule B. Hence, the ratio of binding between the enzyme and nonaggregated inhibitors is 2:1. On the other hand, in the case of aggregated substrates such as membrane phospholipids, the binding ratio has been indicated by kinetics studies to be 1:1. These observations clearly provide evidence of the following phenomena in the catalytic mechanisms of PLA_2s in general and PLA_2 from *D. russelli pulchella* in particular: (i) the lower activity of monodispersed substrates as compared to those of the aggregated ones such as membrane phospholipids, (ii) the lower catalytic activity of PLA_2 from *D. russelli pulchella* as compared to those of other PLA_2s, and (iii) the higher stability of PLA_2 from *D. russelli pulchella* as compared to those of other PLA_2s.

REFERENCES

1. Tsai, L. H., Yang, L. L., and Chang, C. (1980) *Taiwan Kexue 34*, 40−45.
2. Vishwanath, B. S., and Gowda, T. V. (1987) *Toxicon 25*, 929−937.
3. Dennis, E. A. (2000) *Am. J. Respir. Crit. Care Med. 161*, S32−S35.
4. Vadas, P., Stefanski, E., and Pruzanski, W. (1985) *Life Sci. 36*, 579−587.
5. Pruzanski, W., Vadas, P., and Fornasier, V. (1986) *J. Invest. Dermatol. 86*, 380−383.
6. Vishwanath, B. S., Kini, R. M., and Gowda, T. V. (1987) *Toxicon 25*, 501−515.
7. Chandra, V., Nagpal, A., Kaur, P., and Singh, T. P. (1999) *Acta Crystallogr. D55*, 925−926.
8. Lio, Y., and Dennis, E. A. (1998) *Biochim. Biophys. Acta 1392*, 320−332.
9. Chandra, V., Kaur, P., Srinivasan, A., and Singh, T. P. (2000) *J. Mol. Biol. 296*, 1117−1126.
10. Schulze, T. (1996) Ein Echtheitsystem zur Messung der dynamishen Lichtstreuung in flussigkeiten, M.S. Thesis, University Hamburg, Hamburg, Germany.
11. Otwinowski, Z., and Minor, W. (1997) *Methods Enzymol. 176*, 307−326.
12. Chandra, V., Kaur, P., Jasti, J., Betzel, Ch., and Singh, T. P. (2001) *Acta Crystallogr. D57*, 1793−1798.
13. Brünger, A. T., Adams, P. D., Clore, G. M., Delano, W. L., Gros, P., Gorsse-Kunstleve, R. W., Jiang, J. S., Kuszewski, J., Nilges, N., Pannu, N. S., Read, R. J., Rice, L. M., Simonson, T., and Warren, G. L. (1998) *Acta Crystallogr. D54*, 905−921.
14. Jones, T. A., Zou, J.-Y., Cowan, S. W., and Kjeldgaard, W. J. M. (1991) *Acta Crystallogr. A47*, 110−119.
15. Schmitz, K. S. (1990) *An Introduction to Dynamic Light Scattering by Macromolecules*, Academic Press, Boston.
16. Dahneke, B. E. (1983) *Measurement of Suspended Particles by Quasi Elastic Light Scattering*, Wiley, New York.
17. Kasturi, S., and Gowda, T. V. (1989) *Toxicon 27*, 229−237.
18. Kini, R. M. (1997) in *Venom Phospholipase A_2 Enzymes: Structure, Function and Mechanism*, pp 146−147, Wiley, Chichester, U.K.
19. Yuan, W., Quinn, D. M., Sigler, P. B., and Gelb, M. H. (1990) *Biochemistry 29*, 6082−6094.
20. Laskowski, R., Macarthur, M., Moss, D., and Thornton, J. (1993) *J. Appl. Crystallogr. 26*, 283−290.
21. Ramachandran, G. N., and Sasisekharan, V. (1968) *Adv. Protein Chem. 23*, 283−438.
22. Huang, H. C. (1984) *Toxicon 22*, 253−264.
23. Vishwanath, B. S., Kini, R. M., and Gowda, T. V. (1988) *Toxicon 26*, 713−720.
24. Jayanthi, G. P., Kasturi, S., and Gowda, T. V. (1989) *Toxicon 27*, 875−885.
25. Kraulis, P. J. (1991) *J. Appl. Crystallogr. 24*, 946−950.
26. Merritt, E. A., and Murphy, M. E. P. (1994) *Acta Crystallogr. D50*, 869−873.

BI0258593